IIETA International Information and Engineering Technology Association
Advancing the World of Information and Engineering

Traitement du Signal
Vol. 40, No. 3, June, 2023, pp. 895-904
Journal homepage: http://iieta.org/journals/ts

Advanced Optimization of Satellite Image Observation Matrices via Orthogonal Trigonometric Decomposition and Karhunen-Loève Transform

Zeshu Zhang[1*], Shuai Shao[1], Hengyi Lv[1], Hailong Liu[1], Dan Xie[2], Tong Zhang[3]

[1] Changchun Institute of Optics, Precision Mechanics and Physics, Chinese Academy of Sciences, Changchun 130033, China
[2] Asset Management Division, Jilin University, Changchun 130012, China
[3] China Mobile Communications Corporation Jilin Company Ltd, Changchun 130000, China

Corresponding Author Email: zhangzeshu@ciomp.ac.cn

https://doi.org/10.18280/ts.400306

Received: 2 March 2023
Accepted: 10 May 2023

Keywords:
satellite image, observation matrix, QRKL transform

ABSTRACT

Satellite imagery, known for its high resolution and abundant informational content, presents unique opportunities for observation and reconstruction via compressed sensing. Despite the potential, inherent limitations in current compressed sensing observation matrices pose substantial challenges, primarily attributed to pronounced random fluctuations and inadequate robustness. Moreover, these matrices remain unsuccessful in eliminating spectral correlations. To mitigate these challenges, an innovative approach, rooted in Orthogonal Trigonometric Decomposition and Karhunen-Loève Transform, is proposed, hereafter referred to as QRKL. This method demonstrates a marked improvement in optimizing the observation matrix, which is pivotal in compressed sensing specifically in the context of satellite image observation and reconstruction. Experimentally, when applied as the observation matrix, the QRKL transform matrix was observed to significantly enhance the reconstruction quality, stability, and anti-interference capabilities of satellite images. These improvements were noticeably superior compared to those achieved with standard observation matrices such as Gaussian and Bernoulli matrices. Furthermore, the utility of the QRKL optimization method extends beyond specific matrices, demonstrating a broad applicability to traditional observation matrices. This universal application implies that the QRKL method could potentially revolutionize compressed sensing practices in satellite imagery, leading to improved image reconstruction quality. The compelling results of this investigation suggest that QRKL transform-based optimization could provide a novel and powerful tool for advancing satellite imagery compressed sensing methodologies, thereby pushing the boundaries of the current state of the art.

1. INTRODUCTION

Satellite images offer a wealth of information and high resolution, making them valuable in various applications, such as resource detection for oceans, forests, and minerals; real-time monitoring for agriculture, forestry, and animal husbandry; and professional map creation in the field of science and technology [1-6]. However, due to the large volume of data in satellite images and interference from atmospheric clouds, processing and transmitting these images remains a focal point for researchers [7, 8]. As a result, compressed sensing is employed in satellite image processing to observe the extensive image information, sampling the image with fewer data points than Nyquist's theorem requires while maintaining minimal informational redundancy, allowing for complete signal reconstruction [9, 10].

Current research in compressed sensing theory encompasses three main directions: the construction of sparse bases, the creation of observation matrices, and the selection and optimization of recovery algorithms [11-13]. Among these, the design of the observation matrix is crucial for compressed sensing observation of satellite images, as it determines both the compression ratio of the information and the preservation of image information after compression and transmission.

Satellite images collect complex ground information, differing from conventional panchromatic two-dimensional images. The high resolution and wide coverage of satellite images result in a significant increase in data volume, necessitating efficient compressed sensing algorithms and observation matrices tailored to the specific features of satellite images. This ensures not only substantial data compression during transmission but also complete image reconstruction at the receiving end.

Commonly used observation matrices in compressed sensing research include Gaussian random matrix and Bernoulli random matrix [14]. While these observation matrices can effectively reconstruct general two-dimensional images, satellite images present a significantly larger data volume and possess interspectral correlation in addition to spatial redundancy [15]. Employing compressed sensing algorithms with a random matrix as the observation matrix can effectively remove spatial redundancy and achieve signal sparsity due to their perfect randomness. However, interspectral redundancy remains unaffected.

To address this limitation, we propose an optimization method for QRKL observation matrix. This optimized matrix retains the randomness of Gaussian measurement matrix while incorporating the ability of KL transform to effectively remove interspectral correlation in satellite images. The goal is to construct an observation matrix suitable for satellite

image characteristics. The QRKL observation matrix optimization method presented in this paper can increase the maximum value by 2.6-3.3dB, the minimum value by 2.8-3.8dB, and the overall mean value of 50 measurements by approximately 3.5dB, as well as improve the correlation coefficient by about 5%. This results in a reconstructed image that is closer to the original image compared to other measurement matrices.

2. COMPRESSED SENSING THEORY

Compressed sensing breaks the traditional Nyquist theorem on the basis of sparse theory. If the observed signal is sparse or compressible, a low-dimensional observation matrix is set, the signal is projected into the low-dimensional space then the known observation matrix and sparse basis are used to reconstruct the original signal by using the idea of norm approximation. The specific process block diagram is as shown in Figure 1 [16].

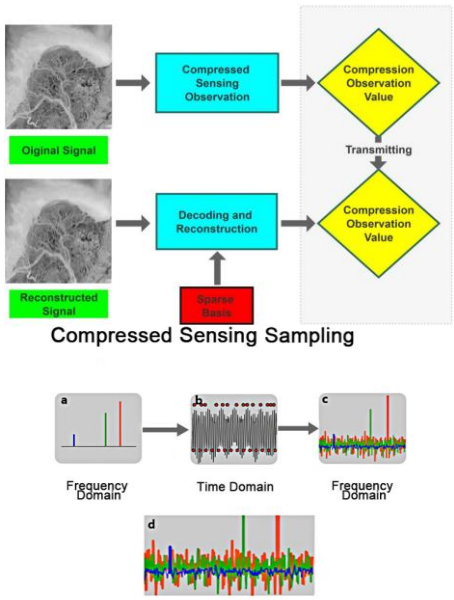

Figure 1. Block diagram of compressed sensing principle

Compressed sensing observation of the signal proceeds as follows the original signal x, length N, and the observation matrix Φ, $M\times N$ dimensional matrix with $M \gg N$. the premise of the compressed sensing observation signal is x sparse, or compressible signal. If x contains k non-zero values, $M \gg K$ and K is called the sparsity of the signal. Ψ is used as sparse training sequence, and the original signal x can be represented by a sparse training sequence Ψ and a set of transformed column vectors θ denoted by.

$$x = \Psi\theta \tag{1}$$

The measurement matrix Φ is used to observe the original signal x and get the measured value y.

$$y = \Phi x \tag{2}$$

Combining above two equations to get

$$y = \Phi x = \Phi\Psi\theta = \Gamma\theta \tag{3}$$

where, $\Gamma=\Phi \cdot \Psi$, the dimension is $M\times N$.

The reconstruction of compressed sensing can be seen as the restoration of the original signal x by using the measured value y, the observation matrix Φ and the training sequence Ψ, using different algorithms. This process can be performed by solving the norm. the transformed column vector of the estimated signal x is obtained

$$\theta_i = \left\langle x, \psi_i \right\rangle (i = 1, 2, \cdots m) \tag{4}$$

θ_i Satisfying the relationship equation

$$\|\theta\|_p \equiv \left(\sum_i |\theta_i|^p \right)^{1/p} \le C \; C > 0 \tag{5}$$

The norm number l_p is an important concept at compressed sensing representing the sparsity of non-zero elements in the solution vector, when the values of p are taken differently, the effects of norm l_p reconstructions will be different. The norm l_0 is commonly used for reconstruction. By solving for norm l_0, the reconstruction process of compressed sensing can be described by the following model.

$$\hat{x} = \arg\min \|x\|_0 \;\; subject \; to \; y = \Phi x \tag{6}$$

There are many kinds of reconstruction algorithms for compressed sensing. Including BP, MP, SP, OMP, SBL, etc. Integrating the performance of various algorithms, we adopt the OMP algorithm as the reconstruction algorithm of compressed sensing for satellite image observation in this paper.

3. QRKL TRANSFORM-BASED OPTIMAL DESIGN FOR SATELLITE IMAGE OBSERVATION MATRIX

The theory of construction of the observation matrix for compressed sensing has been emphasized by researchers. Its design concept was proposed by Candes and Tao [17], the reconstruction signal of compressed sensing is unique and accurate under the condition that the observation matrix satisfies a specific finite isometric constant (Restricted Isometry Constant, RIC). Traditional compressed sensing used Gaussian random matrix at most at most as the observation matrix. The Gaussian random matrix is simple to generate the size of the observation matrix can be adjusted at any time according to the image size. Due to the random generation of matrix the observation matrix is almost completely unrelated to the sparse basis, so it can be reconstructed for any image. However, due to the randomness of Gaussian matrix, the observed signal is easy to affected by external noise and has poor anti-interference capability and no removal for the high-spectral correlation of satellite images. The main idea of this paper is to optimize the Gaussian random matrix by QR decomposition and KL transformation. The QR decomposition preserves the random characteristic part of the Gaussian matrix, so that the optimized matrix still maintains the non-correlation with the sparse basis while satisfying RIP condition, after that the QR optimized matrix is further KL transformed and the nature of the KL transform is used to remove the spectral correlation of satellite image in the observation process principle in as follows.

Our aim is to add the property of removing the inter spectral correlation on the basis of eliminating spatial correlation of traditional Gaussian observation matrix, so that the perfect randomness of Gaussian matrix can not be changed. We first perform QR decomposition on the Gaussian matrix [18], QR decomposition can increase the singular value of the matrix without changing the property if the matrix, namely:

$$\mathrm{A} = \mathrm{QR} \tag{7}$$

This process decomposes the matrix into two parts, Q and R, where Q is an Orthonormal matrix and R is an trigonometric matrix. The QR decomposition of the matrix is calculated linearly as follows

$$\mathrm{Au} = b \Rightarrow (QR)u = b \tag{8}$$

$$Q^{-1}QRu = Q^{-1}b \Rightarrow Ru = Q^{T}b \tag{9}$$

Perform the Gram-Schmidt procedure on each column of matrix A to get orthogonal vectors form $\vec{p}_1, \vec{p}_2, \cdots, \vec{p}_n$, normalize it to get orthonormal vector $\vec{q}_1, \vec{q}_2, \cdots, \vec{q}_n$, Form an orthonormal matrix Q.

$$A = QR \Rightarrow Q^{-1}A = R \tag{10}$$

From the orthogonal matrix property, we may get:

$$R = Q^{-1}A \Rightarrow R = Q^{T}A \tag{11}$$

The precondition that the matrix can be decomposed on QR is that the individual column vectors of A are linearly independent and the Gaussian observation matrix is randomly generated to satisfy this condition. We can decompose QR on Gaussian random matrix. Though QR decomposition we transform the Gaussian random matrix into an upper triangular matrix, which not only get the accurate and stable feature description of Gaussian random matrix, but also retains the random features of Gaussian matrix to the greatest extent, keeping the feature that the Gaussian observation matrix can remove the spatial correlation of the image. In the following, we continue to perform the KL transformation on it.

KL transformation is also called feature vector transformation or Hotelling transformation. It takes the orthogonal matrix composed of the covariance eigenvector of the original data as the transformation matrix to carry out the orthogonal transformation of the original data [19]. It makes most of the covariance matrix of the transformed data to be equal to 0 or approximately equal to 0, except for the diagonal. That is the original inter-pixel spectral correlation is weakened to a large extent [20]. Below, we apply KL-transformation to the upper triangular matrix R transformed by QR in Eq. (11) and the covariance matrix of R is:

$$\mathrm{D}(i,j) = E\left\{(R_i - v_i) \bullet (R_j - v_j)\right\} = E\left\{R_i R_j\right\} - v_i v_j \tag{12}$$

where, $v_i = E\{R_i\}$ is the mean of R_i, since $D(i,j) = D(j,i)$, the covariance matrix D is a real symmetric matrix. For an n order matrix

$$D = \begin{Bmatrix} d_{11} & d_{12} & \cdots & d_{1n} \\ d_{21} & d_{22} & \cdots & d_{2n} \\ \vdots & \vdots & \vdots & \vdots \\ d_{n1} & d_{n2} & \vdots & d_{nn} \end{Bmatrix} \tag{13}$$

The n-dimensional non-zero column vector in the above equation, $\beta = [\beta_1 \quad \beta_2 \quad \cdots \quad \beta_n]^T$. If there is a number γ, such as

$$D\beta = \gamma\beta \tag{14}$$

where, γ is the eigenvalue of matrix D and β is the eigenvector corresponding to the eigenvalue of matrix D, there must be an orthogonal matrix G such that

$$G^T DG = \begin{bmatrix} \gamma_1 & & & 0 \\ & \lambda_2 & & \\ & & \ddots & \\ 0 & & & \gamma_n \end{bmatrix} \tag{15}$$

Taking the above formula, the eigenvalues and eigenvectors of matrix D can be got by iterative method. The eigenvalues are arranged in descending order as follows:

$$|\gamma_1| \geq |\gamma_2| \geq \cdots \geq |\gamma_n| \tag{16}$$

where, n eigenvalues correspond to n eigenvectors, taking them as the basis vector of KL transformation, the transformation matrix of KL can be obtained as follows:

$$T = \begin{vmatrix} \beta_1^T \\ \beta_2^T \\ \vdots \\ \beta_n^T \end{vmatrix} \tag{17}$$

Afterwards, the new matrix obtained by multiplying the transformation matrix T of KL by the matrix R minus the mean, we obtain the result of the KL transformation of the upper triangular matrix R, as shown in the following equation:

$$L = T(R - v) \tag{18}$$

KL is an excellent transformation method in the sense of eliminating the minimum mean square error of correlation in images. In the KL transformation domain of two-dimensional images most of the energy is concentrated on a few transformation coefficients. Therefore, we further transform KL by changing the triangular matrix R after QR transformed and get QRKL+Gaussian matrix, the optimized new observation matrix retains the randomness and non-correlation of Gaussian matrix, which can eliminate the spatial redundancy in data, and has the feature that can reduce the correlation in data spectra, which is especially suitable for CS observation of satellite images.

The QRKL optimization step for the specific observation matrix are as follows:

(1) Input the original satellite image x, judge the image dimension, if x>2, then make the grayscale processing of the image.

(2) Due to the huge amount of data in satellite images x, further imresize scaling of the images are performed.

(3) Set the Fourier transform matrix as the sparse basis Ψ, $\Psi \in R^{N \times N}$, to sparse the image.

(4) Generate a random matrix Φthat matches the standard normal distribution $f(x) = ae^{-(x-b)^2/c^2}$.

(5) The generated Gaussian random matrix $\Phi$is used as the

observation matrix. $\Phi \in R^{M \times N}$, rank $(\Phi)=\omega$, $\omega \leq N$.

(6) The random matrix Φ is QR decomposed $\Phi = \mathrm{QR}$ and the upper triangular matrix R is obtained according to the property of orthogonal transformation $R = Q^T \Phi$.

(7) The matrix R generated by the decomposition of Φ through QR is transformed on KL, according to the Eq. (18), $L = T(R - v)$ and L is used as the optimized observation matrix to observe x.

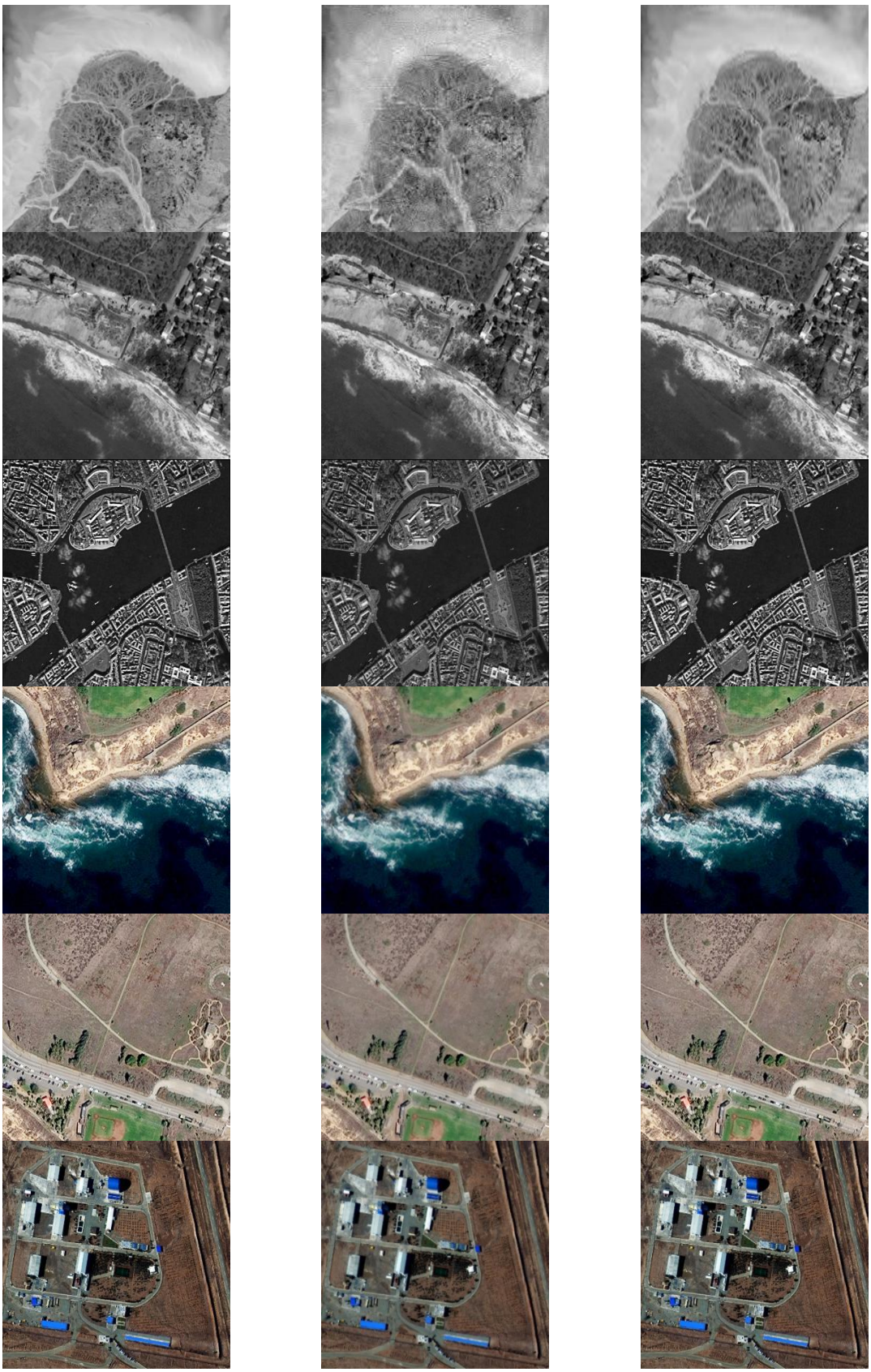

(a) Original satellite

(b) Reconstructed images of Gaussian matrix

(c) Reconstructed images of QRKL+Gaussian matrix

Figure 2. Reconstructed images of satellite images before and after QRKL optimization of Gaussian matrix

4. EXPERIMENTAL SIMULATION AND ANALYSIS

4.1 Effective analysis of QRKL optimized Gaussian matrix on reconstruction quality improvement

In order to verify the effectiveness of the algorithm in this paper we take simulation tests below. The compressed sensing algorithm is used to the construct and analyze the satellite map. The reconstruction algorithm is OMP and the sparse basis is Fourier transform matrix. The observation matrix of compressed sensing adopts the QRKL+Gaussian matrix and Gaussian random matrix in this paper, to observe the original satellite images, the obtained original and reconstructed satellite images are shown in Figure 2(a)-(c).

By comparing the original images with the Gaussian matrix reconstruction, as well as the images optimized by the QRKL method proposed in this paper, it can be known that the reconstructed effect of QRKL+Gaussian random matrix proposed in this paper is more optimized visually than Gaussian random matrix, especially the edges of the Gaussian matrix reconstructed images are very blurred while the detail part of the edges in reconstructed method is clearer in this paper. In order to get the quantitative enhancement effect, for the observation matrix of the compressed sensing, we select more different types of matrices as comparison respectively using six matrices such as Gaussian random matrix, Bernoulli random matrix, part Hadamard matrix sparse random matrix, circulant matrix and QRKL+Gaussian matrix proposed in this paper. And PSNR, the evaluation index of image signal is used for satellite images, the expression is as follows:

$$PSNR = 10\lg\frac{MAXI^2}{MSE} \tag{19}$$

where, MAXI is the maximum gray value of the images, MSE is the mean square error, PSNR(dB) is the maximum peak signal-to-noise ratio, the larger the PSNR value the smaller the transmission loss of satellite image, and the better the reconstruction effect. Figure 3 shows the reconstructed PSNR values obtained from 50 measurements of the six observation matrices.

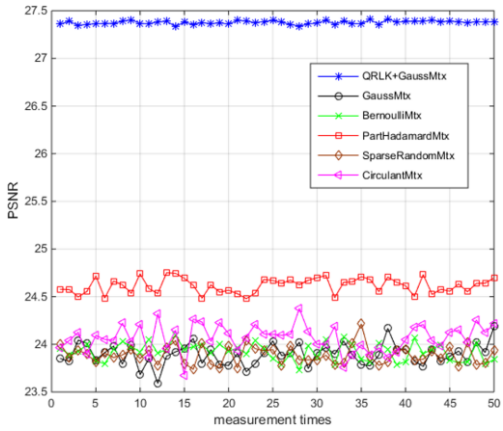

Figure 3. PSNR comparison to 50 times reconstructed images with different observation matrices

From the above figure, it can be known that the reconstruction effect of circulant matrix sparse random matrix, Bernoulli matrix and Gaussian random matrix are similar, and the reconstruction effect of part Hadamard matrix is slightly better and the PSNR is about 0.5-1dB higher than first three matrices. While the QRKL+Gaussian matrix proposed in this paper not only maintains the randomness of Gaussian measurement matrix through QR transformation but also incorporates the features of KL transform which can effectively remove the correlation in satellite image spectra. The CS reconstruction of satellite image is better than the traditional observation matrix reconstruction, and the PSNR is improved about 3.5dB, we have a look at the statistical features analysis of the data reconstructed for 50 times by 6 matrices though Table 1.

Table 1. Statistical features analysis of PSNR data from 50 measurements of different matrices

PSNR	QRKL+Gaussian matrix	Gaussian random matrix	Bernoulli random matrix	part Hadamard matrix	Sparse random matrix	Circulant matrix
Maximum value (dB)	27.42	24.19	24.09	24.75	24.21	24.38
Minimum value (dB)	27.34	23.59	23.73	24.48	23.74	23.68
Mean value (dB)	27.38	23.89	23.93	24.62	23.90	24.07
correlation coefficient	0.9587	0.9074	0.9108	0.9268	0.9117	0.9171
Increase of correlation coefficient	0	5.65%	5.26%	3.44%	5.16%	4.54%

By the statistical features of PSNR including maximum value, minimum value, mean value, and correlation coefficient represent the degree of correlation between the reconstructed images and the original images. When its value is 1, it means the two images are exactly the same. Therefore, the closer the correlation coefficient is to 1, the better the quality of image reconstruction quality is. We can know from the data in table 2 that comparing with the other 5 observation matrices the maximum value and minimum value of the partial QRKL+Gaussian matrix proposed in this paper increase by 2.6-3.3dB, 2.8-3.8dB. The overall mean value for 50 measurements increases by about 3.5dB and the correlation coefficient increases by about 5%, indicating that the reconstructed image of QRKL+Gaussian is closer to the original image than the other measurement matrices. From the statistical results of the data, the improvement in the accuracy of image reconstruction is not accidental, but consistent and systematic. It indicates that the optimization method of QRKL in this paper can reduce the loss of information in satellite images in transmission and improve the reconstructed image quality of satellite images.

4.2 Stability analysis of QRKL optimizing Gaussian matrix in reconstruction effect

In the following, we further analyze the impact of the QRKL optimization method the stability of the system. We take Gaussian matrix and QRKL+Gaussian matrix as measurement matrices to reconstruct the satellite map image for 50 times, while the reconstruction algorithm and sparse basis is

unchanged. Figure 4 shows the average deviation of PSNR reconstructed by the two observation matrices, which can reflect the volatility of the reconstruction effect. From Figure 4 we can see that the average deviation of Gaussian matrix is between 0 and 0.6 dB; while the average deviation of QRKL+Gaussian matrix is between 0 and 0.5. This is due to the addition of QRKL optimization decomposition. Under the premise of maintaining the randomness of Gaussian matrix, the instability generated by random measurement data of Gaussian matrix is greatly eliminated, and its robustness is substantially improved.

Next, we introduce standard deviation and variance to measure the volatility of the data from 50 measurements in different observation matrices. The standard deviation measures the amount of variation in a set of value, low standard deviation means the value size is close to the mean value of the set and high standard deviation means the value range is wide. The variance, on the other hand, is the expected value of the data`s deviation from the square of its mean, it measures the difference between a set of numbers and its mean. Thus, the higher the standard deviation and variance, the greater the volatility of a reconstructed set of data around the mean and it is susceptible to interference. The smaller the standard deviation and variance, the smaller the volatility of the data around the mean, and the more stable the reconstruction effect. Table 2 shows the PSNR variance and standard deviation for 50 measurements of 6 different observation matrices, Gaussian random matrix, Bernoulli random matrix, part Hadamard matrix, sparse random matrix, circulant matrix and QRKL+Gaussian matrix in this paper.

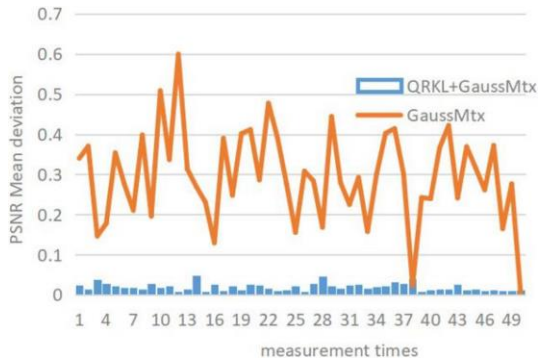

Figure 4. PSNR mean deviation for different observation matrices

Table 2. PSNR variance and standard deviation of the measured data from 6 different observation matrices

Statistical character	QRKL+Gaussian matrix	Gaussian random matrix	Bernoulli random matrix	part Hadamard matrix	Sparse random matrix	Circulant matrix
Variance	2.95×10^{-4}	1.31×10^{-2}	8.17×10^{-3}	6.11×10^{-3}	9.29×10^{-3}	1.96×10^{-2}
Standard Deviation	0.0172	0.1144	0.0904	0.0782	0.0964	0.1399

From the tabular data, it can be known that after 50 times reconstruction of satellite image measurements the variance of Gaussian matrix, Bernoulli matrix, part Hadamard matrix, sparse random matrix and circulant matrix is between $2.95 \times 10^{-2} \sim 6.11 \times 10^{-3}$. the standard deviation is between 0.08 and 0.14. the overall volatility of Gaussian matrix and circulant matrix is the largest and the overall volatility of part Hadamard matrix is the smallest, compared with these traditional matrices, the variance of QRKL+Gaussian matrix proposed in this paper is 2.95×10^{-4}, which is two orders of magnitude lower than the volatility of Gaussian and circulant matrices and one order of magnitude lower than the volatility of the part Hadamard matrix. The standard deviation is also reduced from 0.14 to 0.017. It can be seen that, compared with the conventional observation matrix, the variance and standard deviation of the QRKL matrix for satellite image reconstruction are greatly reduced, the overall fluctuation amplitude is reduced by one order of magnitude which greatly enhances the robustness and improves the ability of signal to resist noise.

4.3 Generalization analysis to the effect of QRKL optimization method on other matrix optimizations

We will still study the optimization effect of the QRKL optimization method on other random matrices. We select the Bernoulli matrix, part Hadamard matrix and circulant matrix as the matrices to be optimized, which are representative of the completely random, partially deterministic and deterministic matrices. We adopt the QRKL method in this paper to optimize the three matrices respectively. Through the comparison of the effect of the three observation matrices to reconstruct satellite images, we analyze the optimization effect of the QRKL optimization method in this paper on other observation matrices except Gaussian random matrix.

Through three observation matrices, namely, Bernoulli matrix part Hadamard matrix and circulant matrix the satellite images reconstructed by CS and the reconstructed image of observation matrix optimized by QRKL are compared as shown in Figure 5 (a)-(f).

From the comparison of the above figures, it can be seen that the construction of the three traditional observation matrices all have grainy edges with lines and blurred details, while the reconstructed images optimized by QRKL have no lines on the visual edge, and the details are clearer. So, the QRKL method proposed in this paper has visual optimization effect on the reconstruction of different observation matrices. Next we further analyze the quantitative PSNR data, and perform QRKL optimization on the Bernoulli matrix, part Hadamard matrix, and circulant matrix respectively, the reconstructed PSNR we obtain from 50 times measurement is shown in Figures 6-8.

From Figures 6-8, it can be seen that the QRKL transform can improve the PSNR about 3.5dB. For Bernoulli matrix, part Hadamard matrix and circulant matrix by optimizing the reconstruction quality of the original satellite image is steadily improved after optimizing these observation matrices by the QRKL transform which indicates that the QRKL optimization method for the conventional observation matrix is generally applicable. From Figure 9, moreover, the original part Hadamard matrices are better optimized for the original images than the Bernoulli matrix and circulant matrix, and the reconstruction results obtained after QRKL transformation are also best for the QRKL+Hadamard matrices at the same time, which the QRKL transformation does not destroy the superior properties from the original observation matrices.

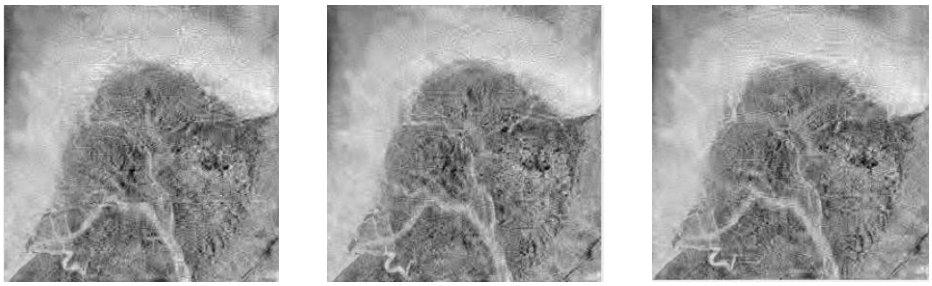

(a) (b) (c)

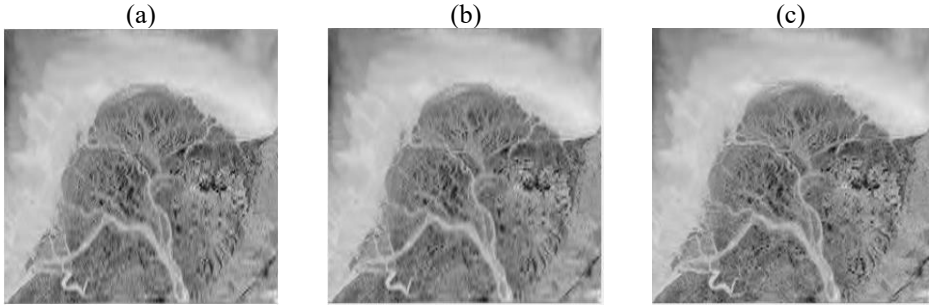

(d) (e) (f)

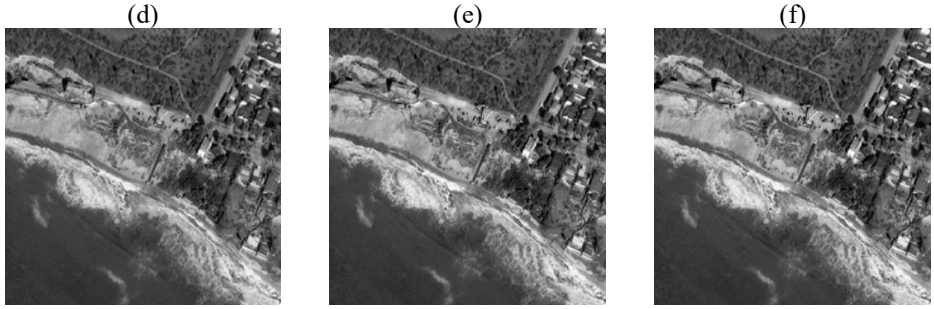

(a) (b) (c)

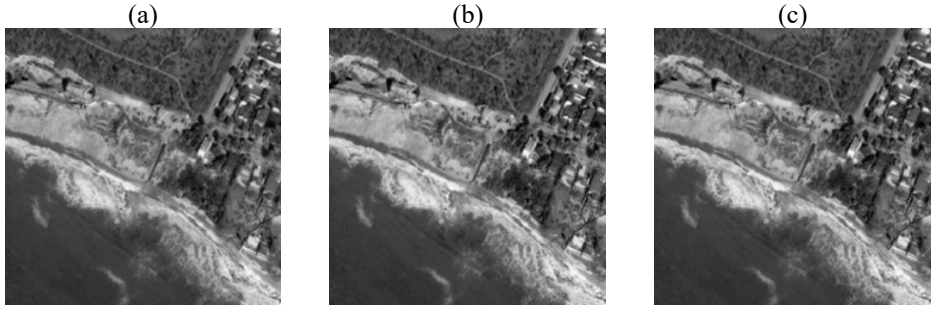

(d) (e) (f)

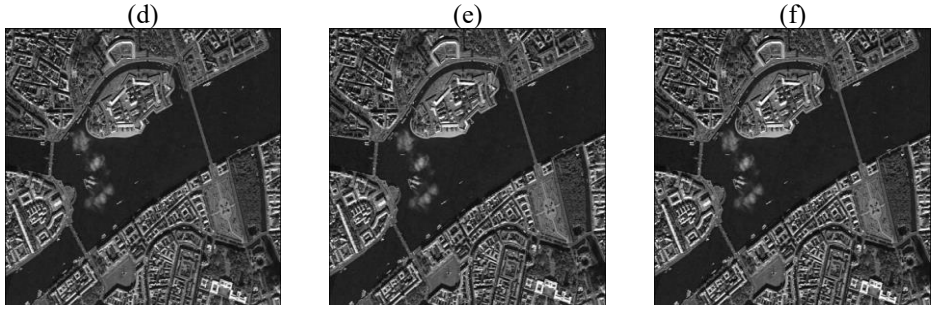

(a) (b) (c)

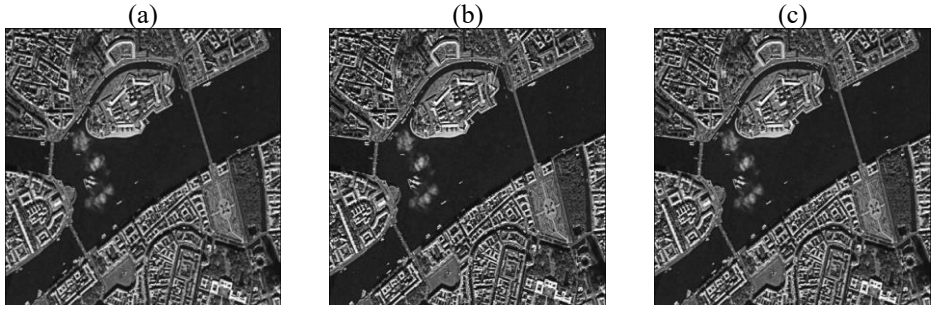

(d) (e) (f)

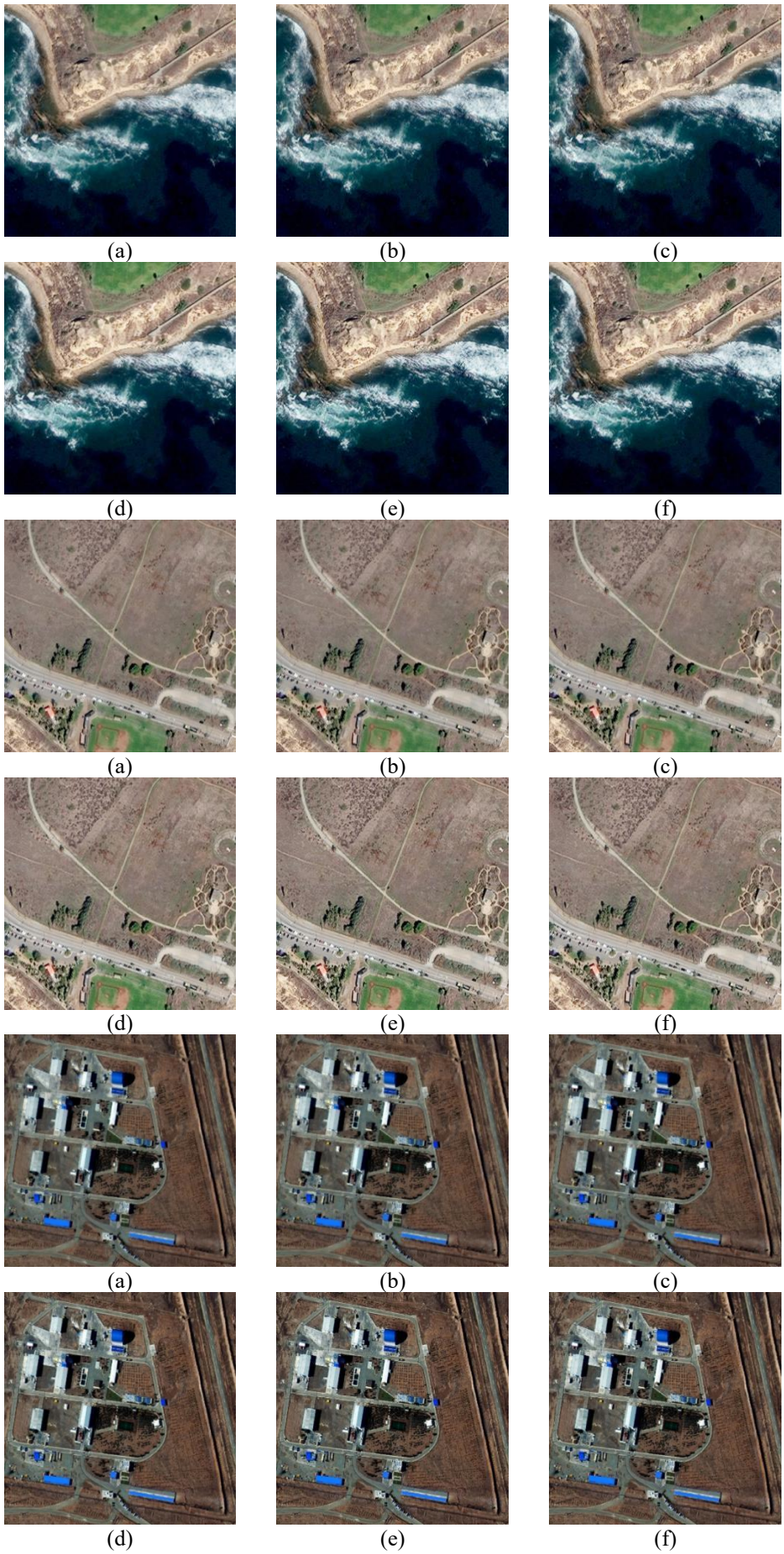

Figure 5. Reconstructed images in satellite images before and after optimization by QRKL for 3 different observation matrices (a) Bernoulli matrix; (b) Part Hadamard matrix; (c) Circulant matrix; (d) QRKL+Bernoulli matrix; (e) QRKL+part Hadamard matrix; (f) QRKL+circulant matrix

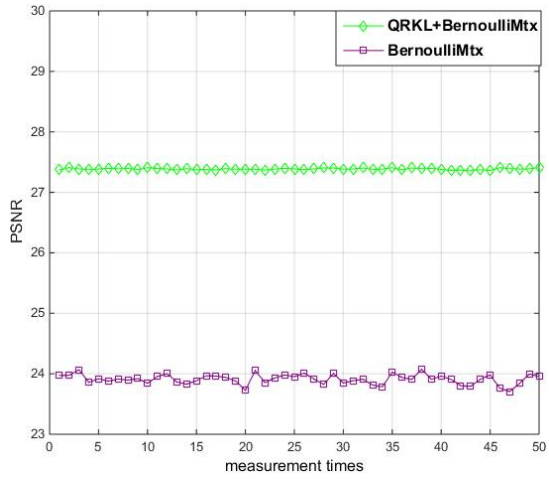

Figure 6. The comparison of the effect on Bernoulli observation matrix optimization for QRKL transformation

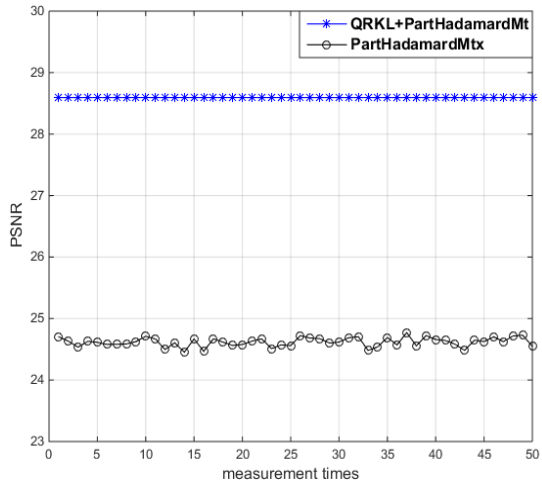

Figure 7. The comparison of the effect on part Hadamard observation matrix optimization for QRKL transformation

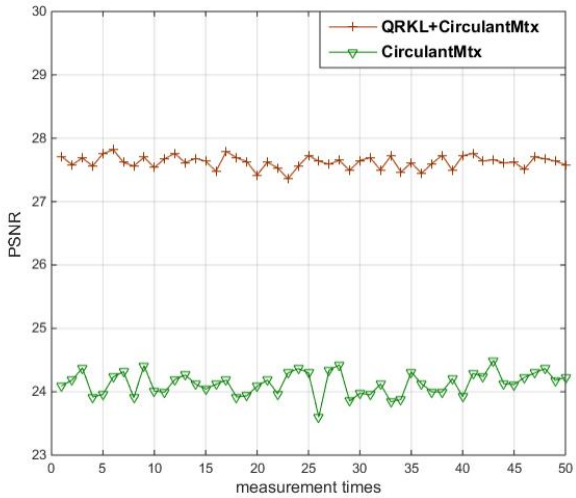

Figure 8. The comparison of the effect on circulant observation matrix for QRKL transformation

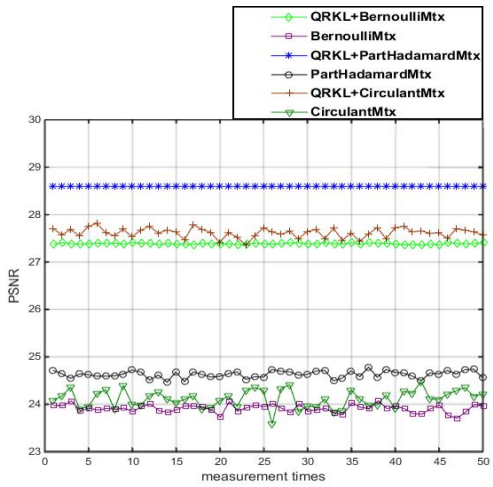

Figure 9. The comparison of the effect on observation matrix for QRKL transformation

5. CONCLUSION

In this study, the advantages of QR transform and KL transform are combined in a proposed observation matrix optimization method based on QRKL transform. By taking the QRKL transform matrix as the compressed sensing observation matrix, satellite images with multiple correlation features are observed and reconstructed. Experimental results indicate that, when compared to commonly used observation matrices such as Gaussian matrix, Bernoulli matrix, part Hadamard matrix sparse random matrix, and circulant matrix, the QRKL transform matrix improves the PSNR of the reconstructed image by approximately 3.5 dB and enhances the accuracy of satellite image reconstruction by 14.6%. Additionally, the fluctuation amplitude of data is reduced from 0.14 to 0.017. These findings suggest that the QRKL transform matrix not only improves the reconstruction quality of satellite images but also enhances the stability and noise resistance of the signal.

While the QRKL optimization method appears to be universally applicable to conventional observation matrices, the KL transform lacks a fixed basis and has a complex algorithm with intensive computing requirements. Further research is needed on reducing the operational complexity and improving hardware technology development to make the implementation of the algorithm in hardware feasible.

FUNDING

This research was funded by National Natural Science Foundation of China (Grant No.: 62005269).

REFERENCES

[1] Ondulo, J.D., Kalande, W. (2006). High spatial resolution satellite imagery for PID improvement in Kenya. In Proceedings of the FIG Congress: Shaping the Change, Munich, Germany.

[2] Hwang, J.T., Chang, K.T., Chiang, H.C. (2011). Satellite image classification based on Gabor texture features and SVM. In 2011 19th International Conference on Geoinformatics, Shanghai, China, pp. 1-6. https://doi.org/10.1109/GeoInformatics.2011.5980774

[3] Karwowska, K., Wierzbicki, D. (2022). Using super-resolution algorithms for small satellite imagery: A systematic review. IEEE Journal of Selected Topics in Applied Earth Observations and Remote Sensing, 15: 3292-3312. https://doi.org/10.1109/JSTARS.2022.3167646

[4] Dai, L., Rizos, C., Wang, J. (2001). The role of pseudo-satellite signals in precise GPS-based positioning. Journal of Geospatial Engineering, 3(1): 33-44.

[5] Mansourifar, H., Moskowitz, A., Klingensmith, B., Mintas, D., Simske, S.J. (2022). GAN-based satellite imaging: A survey on techniques and applications. IEEE Access, 10: 118123-118140. https://doi.org/10.1109/ACCESS.2022.3221123

[6] Zi, Y., Xie, F., Zhang, N., Jiang, Z., Zhu, W., Zhang, H. (2021). Thin cloud removal for multispectral remote sensing images using convolutional neural networks combined with an imaging model. IEEE Journal of Selected Topics in Applied Earth Observations and Remote Sensing, 14: 3811-3823. https://doi.org/10.1109/JSTARS.2021.3068166

[7] Candes, E.J., Tao, T. (2006). Near-optimal signal recovery from random projections: Universal encoding strategies?. IEEE Transactions on Information Theory, 52(12): 5406-5425. https://doi.org/10.1109/TIT.2006.885507

[8] Syrris, V., Ferri, S., Ehrlich, D., Pesaresi, M. (2015). Image enhancement and feature extraction based on low-resolution satellite data. IEEE Journal of Selected Topics Applied Earth Observations and Remote Sensing, 8(5): 1986-1995. https://doi.org/10.1109/JSTARS.2015.2417864

[9] Luo, S., Guo, Q., Zhao, H., et al. (2017). Noise reduction of swept-source optical coherence tomography via compressed sensing. IEEE Photonics Journal, 10(1): 1-9. https://doi.org/10.1109/JPHOT.2017.2787662

[10] Zhang, S., Wu, J., Chen, D., Li, S., Yu, B., Qu, J. (2018). Fast frequency-domain compressed sensing analysis for high-density super-resolution imaging using orthogonal matching pursuit. IEEE Photonics Journal, 11(1): 6900108. https://doi.org/10.1109/JPHOT.2018.2884730

[11] Chen, J., Hu, T., Luo, Q., et al. (2023). Improved U-Net3+ with spatial–spectral transformer for multispectral image reconstruction. IEEE Photonics Journal, 15(2): 7800511. https://doi.org/10.1109/JPHOT.2023.3236810

[12] Wu, J., Wang, J., Hu, L. (2022). Sequential subtraction-based compressive single-pixel imaging in complicate ambient light. IEEE Photonics Journal, 14(6): 7864007. https://doi.org/10.1109/JPHOT.2022.3229664

[13] Lei, X., Ma, X., Yang, Z., Peng, X., Li, Y., Zhao, M., Fan, M. (2021). Improving compressed sensing image reconstruction based on atmospheric modulation using the distributed cumulative synthesis method. IEEE Photonics Journal, 13(5): 7800107. https://doi.org/10.1109/JPHOT.2021.3108194

[14] Tsaig, Y., Donoho, D.L. (2006). Extensions of compressed sensing. Signal processing, 86(3): 549-571. https://doi.org/10.1016/j.sigpro.2005.05.029

[15] Baraniuk, R.G., Cevher, V., Duarte, M.F., Hegde, C. (2010). Model-based compressive sensing. IEEE Transactions on Information Theory, 56(4): 1982-2001. https://doi.org/10.1109/TIT.2010.2040894

[16] Cao, H., Liu, Q., Wu, Y. (2020). Transform domain: design of closed-form joint 2-D DOA estimation based on QR decomposition. Circuits, Systems, and Signal Processing, 39: 5318-5329. https://doi.org/10.1007/s00034-020-01416-8

[17] Candes, E.J., Tao, T. (2005). Decoding by linear programming. IEEE Transactions on Information Theory, 51(12): 4203-4215. https://doi.org/10.1109/TIT.2005.858979

[18] Lee, H., Yoon, S., Loohuis, P., Hong, J.H., Kang, S., Choi, W. (2022). High-throughput volumetric adaptive optical imaging using compressed time-reversal matrix. Light: Science & Applications, 11(1): 16. https://doi.org/10.1038/s41377-021-00705-4

[19] Ni, B.Y., Jiang, C., Li, J.W., Tian, W.Y. (2020). Interval KL expansion of interval process model for dynamic uncertainty analysis. Journal of Sound and Vibration, 474: 115254. https://doi.org/10.1016/j.jsv.2020.115254

[20] Yu, X.C., Zhi, Y., Tang, S.J., Li, B.B., Gong, Q., Qiu, C.W., Xiao, Y.F. (2018). Optically sizing single atmospheric particulates with a 10-nm resolution using a strong evanescent field. Light: Science & Applications, 7(4): 18003. https://doi.org/10.1038/lsa.2018.3